

Numerical study of grid turbulence in two dimensions and comparison with experiments on turbulent soap films

C. H. Bruneau,¹ O. Greffier,² and H. Kellay²

¹*Mathématiques Appliquées de Bordeaux, U. Bordeaux I, 351 Cours de la Liberation, 33405 Talence Cedex, France*

²*Centre de Physique Moléculaire Optique et Hertzienne, U. Bordeaux I, 351 Cours de la Liberation, 33405 Talence Cedex, France*

(Received 15 June 1998; revised manuscript received 9 April 1999)

Numerical simulations of two dimensional channel flow behind an array of cylinders are carried out for high Reynolds numbers. Results for the energy density and enstrophy spectra, as well as for velocity and vorticity differences, are presented. The results compare favorably with recent experiments carried out with turbulent soap films. Some marked deviations from expected behavior are found for the enstrophy spectrum and for moments of vorticity increments. [S1063-651X(99)51608-5]

PACS number(s): 47.27.Gs, 47.11.+j, 47.27.Jv, 92.60.Ek

Two dimensional (2D) turbulence is different from three dimensional (3D) turbulence. The absence of vortex stretching in 2D leads, in the presence of small dissipation, to the conservation of both enstrophy (mean squared vorticity) and energy. While theories of 3D turbulence suggest a direct cascade of energy from the scale of injection to smaller scales, the theories of 2D turbulence suggest an inverse cascade of energy from small to large scales. On the other hand a direct cascade of enstrophy from large to small scales is expected [1–3]. This picture of 2D turbulence has received some confirmation from numerical simulations [4–6]. Recent experiments using soap films as model 2D systems for the study of decaying grid turbulence have produced several results, some of which deviate from expected behavior. The purpose of this work is to test whether these deviations can also be seen in an ideal 2D fluid by carrying out direct numerical simulations of grid turbulence in two dimensions. A difficulty with soap films is that they can sustain thickness fluctuations, which can render the flow compressible. Experiments on 2D decaying turbulent flows use rapidly flowing soap films driven by gravity in vertical channels [7,8]. These experiments follow some pioneering work by Couder *et al.* [9], and Gharib and Derango [10], who used soap films to study 2D hydrodynamics. The flow is perturbed by an array of cylinders or grid placed perpendicular to the film plane; nearly isotropic turbulence is obtained some distance behind the grid. Although the results seem to be consistent with expectations for 2D decaying turbulence [11], the enstrophy spectra [12] and the measurements of velocity differences revealed some unusual features [13].

Here we study numerically the flow in a 2D channel where an array of cylinders perturbs the flow in a similar fashion as in experiments. The flow is studied for Reynolds numbers (based on the cylinder diameter) as high as 5×10^5 : at least two orders of magnitude higher than the experimental Reynolds numbers. To our knowledge, these are the first direct numerical simulations of high Reynolds number grid turbulence in two dimensions. The results are in good agreement with the experiments, showing that soap films are good models for 2D hydrodynamics. Our study extends the experimental results to high Reynolds numbers and to small enough scales to probe the dissipation range. As

far as we know, the dissipative range of 2D turbulence remains elusive. Our results show that the vorticity differences between two points depend on the scale, which is not expected from the classical scaling and points to an anomalous behavior for 2D turbulence. Also, the spectra of both the enstrophy and the energy are cut off by an exponential decrease at high wave numbers where dissipation becomes important.

The Navier-Stokes equations for an incompressible fluid are numerically solved for the channel geometry. Our numerical simulations take advantage of recent studies on incorporating obstacles and boundary conditions in incompressible 2D flows [14]. The highest resolution of our simulations was $640 \times (3 \times 640)$. The time step is 10^{-4} and the runs had typical durations of at least 10^6 time steps. We fix the channel width to 1, the channel length to 3, the mean velocity to 1, and vary the viscosity to achieve different Reynolds numbers (Re). The diameter of the cylinders is 0.1 and the spacing between the cylinders is 0.2. There are five cylinders in the array or grid. These dimensions resemble the experimental conditions.

Figure 1 shows a visualization of the vorticity contours behind the grid placed at a length of one from the entrance for $Re=5 \times 10^5$. The flow before the grid is laminar. After the grid, the flow is dominated by the presence of vortices interacting very strongly with each other. There are strong vorticity gradients which are well captured by the presence of dark regions in the contour plot. On average, the size of the vortical structures, advected downstream from the grid, seems to grow as the distance from the grid increases.

Since, in experiments, the measured quantities are time traces, we performed a similar analysis of our data; a time trace was recorded at different positions of the flow and Fourier analyzed to yield the power spectrum. This is done for the longitudinal u and transverse v components of the velocity, as well as for the vorticity w . Typical results for $Re=5 \times 10^5$ are shown in Fig. 2. The spectra for the two components of the velocity at a location of one channel width from the grid have roughly similar amplitudes in the frequency range studied; the turbulence is nearly isotropic at this location. Similar results were obtained at other locations. Both

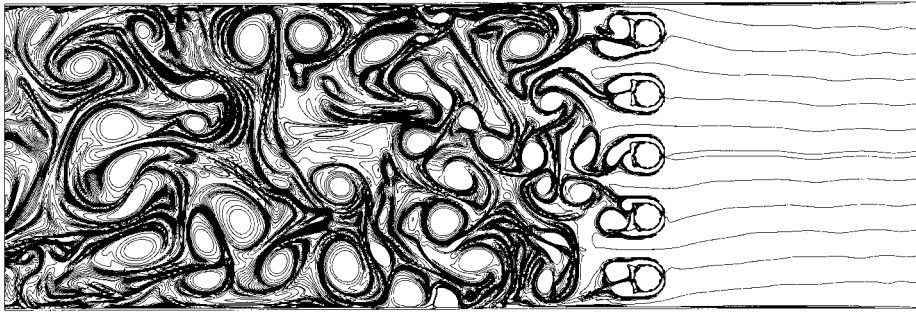


FIG. 1. Vorticity contours in the 2D channel perturbed by a horizontal array of cylinders or grid. The cylinder diameter is 0.1, the length of the channel is 3 and its width is 1 ($Re=5 \times 10^5$).

spectra show a continuous decrease as the frequency is increased with a small flat part at small frequencies. A steeper decrease is observed at high frequencies. The whole spectrum (except at low frequencies) can be fit to the following functional form: $f^{-\beta} \exp(-f/f_0)$. The cutoff frequency f_0 is 18. The exponent β is close to 3.7, in agreement with results from experiments on turbulent soap films [7,8]. However, the steep decrease of the spectrum at high frequencies has not been seen in experiments. We believe the simulations capture the dissipative range. Our finding that the steep decrease is exponential at high frequencies resembles results from 3D turbulence experiments where an exponential decrease was also evidenced [15].

In Fig. 2 we also show the results for the enstrophy spectrum. This spectrum flattens at frequencies below about 4 Hz. Above this frequency, the amplitude of the spectrum decreases as the frequency increases. This decrease is steeper at high frequencies. As for the velocity power spectra, the enstrophy spectrum can be approximated by a product of a power law and an exponential with an exponent γ close to 1.9 and a cutoff frequency of 18. The exponent is also in agreement with the measured exponent in the soap film experiments [12]. In the experiments no sign of the steep decrease was observed.

We use the Taylor frozen turbulence assumption (which assumes that the eddies are swept by the mean flow past the observation point without much change in their structure) to

convert the frequency to a wave number k_y (k_y is the longitudinal component of the wave vector \mathbf{k} and y is the coordinate in the flow direction); $k_y = 2\pi f/V$, where V is the mean speed. Using this conversion, a frequency of 1 corresponds to the channel width L ; the highest frequency in the graph corresponds to $L/500$. Using this assumption, the velocity power spectra and the enstrophy spectra scale with the wave number in the same way as they scale with the frequency. From these one dimensional spectra, the scaling of the velocity power spectra or, equivalently, the energy density spectrum, seems to be consistent with predictions of the phenomenological theories of 2D turbulence, which predict a scaling law for these spectra with an exponent β of 3 in the enstrophy cascade range. A similar conclusion was made in the soap film experiments. However, the exponents from experiments and from our simulation are systematically higher than 3. Now the enstrophy scaling shows stronger deviation from theoretical expectations. The expected exponent γ is 1, while we measure an exponent close to 2. A similar exponent was observed in experiments [12]. We have no explanation for this discrepancy with the theoretical expectations. As for the exponential correction to the spectra at high frequencies or small scales, we know of no predictions for 2D turbulence. This correction, however, is similar to the 3D case. Note that the cutoff frequency for the exponential decrease corresponds to a length scale $L/18$ which would be related to the scale at which viscous dissipation is important. In the

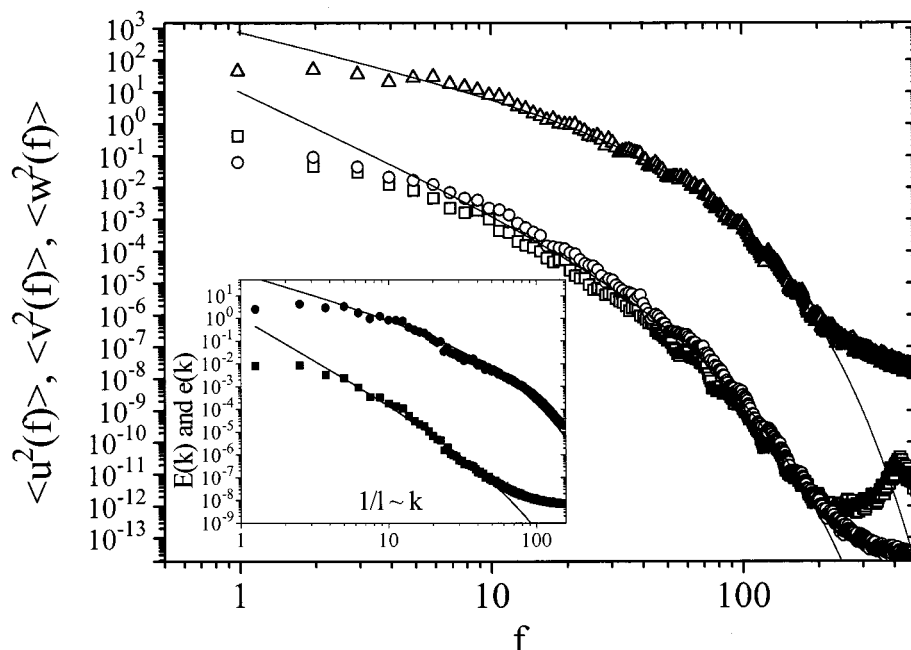


FIG. 2. Longitudinal (squares) and transverse (circles) velocity power spectra at a distance of 1 from the grid ($Re=5 \times 10^5$). Enstrophy spectrum (triangles) for the same flow. These spectra are obtained from time series. The solid lines are fits to the data (see the text for functional form). Inset: energy density (squares) and enstrophy (circles) spectra as obtained from 2D Fourier transforms of the velocity and vorticity fields ($Re=5 \times 10^5$). The solid lines are fits to the data using the functional form given in the text.

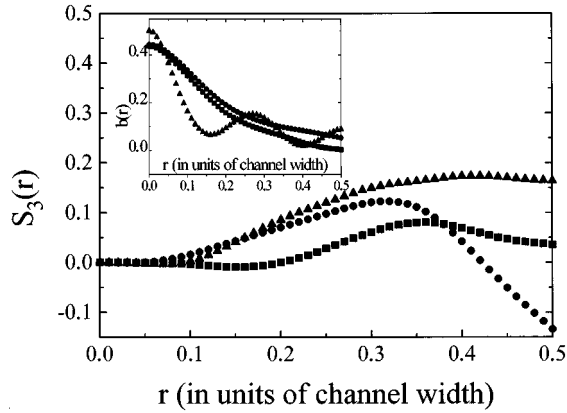


FIG. 3. Third moment of the longitudinal velocity difference for $Re=10^4$ (squares), 5×10^4 (triangles), and 5×10^5 (filled circles). The increment is in units of channel width fixed to 1. All of the moments are calculated for a distance of 1 from the grid. Inset: $b(r)$ calculated at different locations Y from the grid; $Y=0.4$ (triangles), 1 (squares), and 1.2 (filled circles) for $Re=5 \times 10^4$.

absence of a theoretical prediction for this exponential decrease, we are unable to determine the dissipative scale.

The inset to Fig. 2 shows the energy density $E(k)$ and enstrophy $e(k)$ spectra obtained from 2D Fourier transforms of the 2D velocity and vorticity fields for a square of size $0.8L$ near the outlet of the channel. The result gives the k (the wave vector modulus) dependence of these quantities directly. These spectra have roughly similar shapes as the spectra obtained from the time series. Note that a spatial image of the flow field contains contributions from different locations from the grid. Since the flow evolves as a function of distance from the grid, these different locations suffer from the decay of the turbulence in different ways. Nonetheless, both the enstrophy and energy spectra can be reasonably fit to a product of a power law and an exponential function as for the one dimensional frequency spectra. The parameters for the fit are a cutoff length $L/22$ and exponents of 3.7 and 1.9 for the energy and enstrophy spectra, respectively.

Let us focus on the moments of longitudinal velocity and vorticity differences across a scale r . These are defined as $\delta u^n(r) = \langle [u(y+r) - u(y)]^n \rangle$ and $dw^n(r) = \langle [w(y+r) - w(y)]^n \rangle$, with r in the longitudinal direction y , and the brackets indicate a time or ensemble average. These differences are calculated from the time series by taking a variable time increment τ . By using the frozen turbulence assumption one can identify τ with a distance $r = V\tau$. We follow this procedure since the experiments are carried out in the same way, which allows us to compare our results to experiment directly. Some typical results are shown in Fig. 3 for the third moment of longitudinal velocity differences defined as $S_3(r) = \delta u^3(r)$. Three runs with Re of 10^4 , 5×10^4 , and 5×10^5 are displayed. For the lower Reynolds number $S_3(r)$ starts out small but negative at small r , goes through a minimum, and starts to increase going to positive values at larger r before it decreases. A similar result is obtained for higher Re . The difference is mostly seen at small scales where the minimum seen previously is much less visible. At larger r , $S_3(r)$ starts to decrease and becomes negative for $Re=5 \times 10^5$. Both the small minimum and the positive part are seen in experiments on flowing soap films as well as the

maximum in the curve at larger separations [13]. Exact calculations starting from the Navier-Stokes equations show that $S_3(r)$ in 3D follows (Kolmogorov's $-4/5$ law): $S_3(r) = -4/5 \varepsilon r + 6\nu dS_2/dr$. ε is the energy dissipation rate and ν is the kinematic viscosity. $S_2(r)$ is the second moment of the velocity difference. The 2D equivalent of this law is $S_3(r) = -3/2 \varepsilon r + 6\nu dS_2/dr$. For decaying turbulence, as is the case with our simulations, the above relation has to be completed with a term that accounts for the decay of $S_2(r)$. This relation can be written as $S_3(r) = 6/r^3 \int_0^3 db(z,t)/dt dz$, where $b(r,t) = \langle u(y+r,t)u(y,t) \rangle$ is the longitudinal velocity correlation function [13]. Here we neglect dissipation. We then identify the downstream distance from the grid Y with the time of evolution t using $Vt=Y$. As can be seen in the inset to Fig. 3, the $b(r)$ measured at a distance of 0.4 from the grid is larger than the $b(r)$ measured at a distance of 1 for the small scales, but the latter $b(r)$ becomes larger at larger scales. At a distance of 1.2, $b(r)$ is also larger at large scales than its equivalent at a distance of 1. The above expression for $S_3(r)$ is therefore consistent with our results, as the derivative of $b(r)$, with respect to time or downstream distance, would change sign from negative at small r to positive at larger r , as seen in both experiments and our simulations. Note that a positive $S_3(r)$ supports the idea that energy cascades from small scales to large scales in stark contrast to

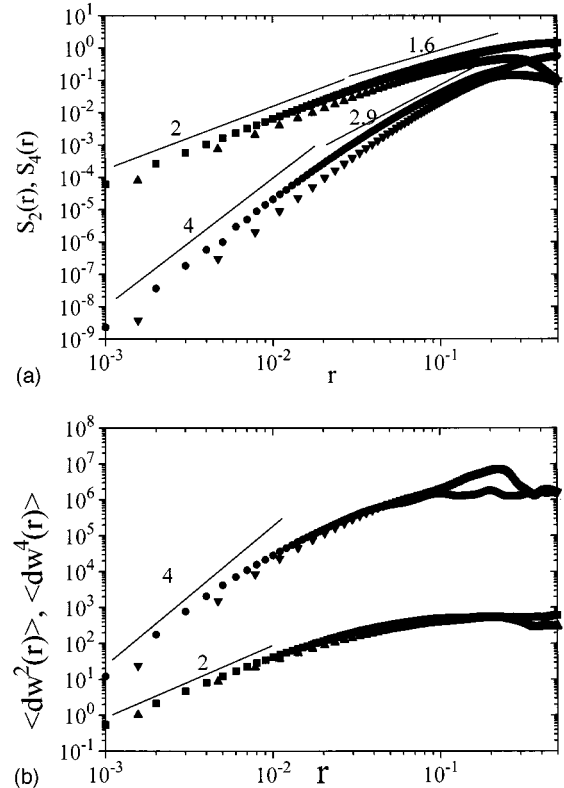


FIG. 4. (a) Second (squares) and fourth (circles) moments of longitudinal velocity differences with an increment r in the flow direction (for a distance of 1 from the grid). Second (triangles) and fourth (down triangles) moments of transverse velocity differences with an increment r in the transverse direction. (b) second (squares) and fourth (circles) moments of vorticity differences with r in the longitudinal direction; second (triangles) and fourth (down triangles) moments of vorticity differences with r in the transverse direction. $Re=5 \times 10^5$.

3D turbulence [16] and, despite the fact, the energy scaling indicates that the turbulence is in the enstrophy cascade range of scales. A similar observation was made recently [6].

Figure 4(a) shows the second and fourth moments of longitudinal velocity increments. Note that these moments follow approximately a dependence of the form $\delta u^n(r) \approx r^{a_n}$. In the enstrophy cascade range, theory predicts $a_n = n$. The exponents a_n are difficult to determine in our case but appear slightly smaller than n in the range of scales between $L/10$ and $L/50$. This is presumably due to the extent of the inertial range as was pointed out in [17]. This dependence saturates at large scales starting at about $L/4$. In experiments, the results for the second and fourth moments of absolute values of the longitudinal velocity increments showed exponents of 1.6 and 2.9, respectively, which are close to the ones found numerically. At smaller scales (less than $L/40$), however, we observe a scaling of the form r^n for the moments of order n . This variation is expected on the grounds of the analyticity of the structure functions [15] in the dissipative range. Again, this has not been seen in experiments yet. In Fig. 4(a) we also show the second and fourth moments of the transverse velocity difference ($\delta v^n(r) = \langle [v(x, r) - v(x)]^n \rangle$ for $n = 2$ and 4) with the increment r taken in the transverse direction x . This calculation uses the values of the transverse velocity along a line perpendicular to the flow direction. These moments follow the same functional form as the moments of the longitudinal velocity differences. However, the amplitude of the transverse moments is slightly smaller than the longitudinal moments. This points to the fact that the turbulence is not perfectly isotropic with fluctuations along the flow direction being somewhat larger than transverse fluctuations. This difference is even larger at large scales where it is probably due to the presence of boundaries.

Figure 4(b) shows the second and fourth moments of vorticity increments $dw(r)$. Here we show results for r in the flow direction and for r perpendicular to the flow direction. The moments for the two directions of the increment r have

roughly equal amplitudes, but at small scales the moments along the transverse direction are slightly smaller than their counterparts for a longitudinal increment. These moments show a roughly flat part at large scales starting at about $L/10$. At smaller scales the moments decrease as the distance decreases. The decrease does not follow a clear scaling law as a function of r . The fact that these moments show a dependence on the scale is consistent with the higher exponent for the enstrophy spectrum and indicates deviations from the expected behavior for the enstrophy cascade range of scales where they are expected to be flat as the separation r changes. In this respect, it is interesting to note that recent theory puts a bound on the variation of $dw^2(r)$ only where it was found that the variation is of the form $r^{2/3}$ or weaker [18]. Our data indicate that this bound is roughly obeyed. For a separation r smaller than $L/50$, the vorticity increments show a steeper decrease as the scale decreases. While the range is small, this decrease is consistent with an r^n dependence for the moments of order n just as for the moments of velocity increments. Again this may be a sign that these small scales lie in the dissipative range.

To summarize, we present new results from a numerical simulation of two dimensional grid turbulence concerning energy and enstrophy spectra, and the moments of velocity and vorticity increments. Our results are in good agreement with experiments on turbulent soap films and extend them to higher Reynolds numbers and small enough scales to evidence the dissipative range. The results indicate an anomalous behavior of the enstrophy spectra and vorticity increments at small scales. The third moment of velocity increments is in agreement with the experimental results and shows a non-negligible positive part, which is consistent with exact calculations and can be attributed to the decaying nature of the turbulence generated.

We are grateful to W. I. Goldburg, X. L. Wu, and A. Belmonte for many discussions.

-
- [1] R. Kraichnan, *Phys. Fluids* **10**, 1417 (1967).
 - [2] G. K. Batchelor, *Phys. Fluids Suppl. II* **12**, 233 (1969).
 - [3] M. Lesieur, *Turbulence in Fluids*, 2nd ed. (Kluwer, Dordrecht, 1990).
 - [4] M. E. Brachet, M. Meneguzzi, and P. L. Sulem, *Phys. Rev. Lett.* **57**, 683 (1986).
 - [5] L. M. Smith and V. Yakhot, *Phys. Rev. Lett.* **71**, 352 (1993).
 - [6] V. Borue, *Phys. Rev. Lett.* **71**, 3967 (1993); **72**, 1475 (1994).
 - [7] H. Kellay, X-I. Wu, and W. I. Goldburg, *Phys. Rev. Lett.* **74**, 3975 (1995).
 - [8] B. K. Martin, X. L. Wu, W. I. Goldburg, and M. H. Rutgers, *Phys. Rev. Lett.* **80**, 3964 (1998).
 - [9] Y. Couder, *J. Phys. (France) Lett.* **45**, L-353 (1984); Y. Couder *et al.*, *Physica D* **37**, 384 (1989).
 - [10] M. Gharib and P. Derango, *Physica D* **37**, 406 (1989).
 - [11] J. R. Chasnov, *Phys. Fluids* **9**, 171 (1997).
 - [12] H. Kellay, X. L. Wu, and W. I. Goldburg, *Phys. Rev. Lett.* **80**, 277 (1998).
 - [13] A. Belmonte *et al.*, *Phys. Fluids* **11**, 1196 (1999).
 - [14] Ph. Angot, C. H. Bruneau, and P. Fabrie, *Numer. Math.* **81**, 497 (1999); C. H. Bruneau and P. Fabrie, *Math. Modell. Numer. Anal.* **30**, 815 (1996); *Int. J. Numer. Methods Fluids* **19**, 693 (1994); C. H. Bruneau and C. Jouron, *J. Comp. Phys.* **89**, 389 (1990); C. H. Bruneau, *Comp. Fluid Dyn. Rev.* **1**, 114 (1998).
 - [15] L. Sirovich, L. Smith, and V. Yakhot, *Phys. Rev. Lett.* **72**, 344 (1994).
 - [16] S. I. Vainshtein and K. R. Sreenivasan, *Phys. Rev. Lett.* **73**, 3085 (1994).
 - [17] A. Babiano, C. Basdevant, and R. Sadourny, *J. Atmos. Sci.* **42**, 941 (1985).
 - [18] G. L. Eyink, *Phys. Rev. Lett.* **74**, 3800 (1995).